Further study of $f_0(1710)$ with the coupled-channel approach and the hadron molecular picture

Zheng-Li Wang[1,2,*] and Bing-Song Zou[1,2,3,†]

[1]*CAS Key Laboratory of Theoretical Physics, Institute of Theoretical Physics, Chinese Academy of Sciences, Beijing 100190, China*
[2]*School of Physics, University of Chinese Academy of Sciences (UCAS), Beijing 100049, China*
[3]*School of Physics and Electronics, Central South University, Changsha 410083, China*

(Received 8 August 2021; accepted 12 November 2021; published 1 December 2021)

The $f_0(1710)$ was previously proposed to be a dynamically generated state with interactions between vector mesons. We extend the study of $f_0(1710)$ by including its coupling to channels of pseudoscalar mesons within the coupled-channel approach. The channels involved are $K^*\bar{K}^*, \rho\rho, \omega\omega, \phi\phi, \omega\phi, \pi\pi, K\bar{K}, \eta\eta$. We show that the pole assigned to $f_0(1710)$ does not change much. Then we calculate the partial decay widths of $f_0(1710) \to K^*\bar{K}^* \to \pi\pi, K\bar{K}, \eta\eta$ as the coupled channel dynamically generated state as well as assuming it to be a pure $K^*\bar{K}^*$ molecule. In both cases the ratios of partial decay widths agree fairly with that in PDG.

DOI: 10.1103/PhysRevD.104.114001

I. INTRODUCTION

More and more hadron resonances have been proposed to be hadron molecules [1] with much more predicted ones to be searched for [2]. Among various approaches for studying hadron molecules, a quite popular one is the unitary extension of chiral perturbation theory, which has been successful in studying the meson-baryon and meson-meson interactions at low energy [3–10]. A well-known example is the $\Lambda(1405)$ [11], which can be dynamically generated in the vicinity of the $\pi\Sigma$ and $K^- p$ thresholds. The another example is $f_0(980)$ [8,12], which is considered to arise due to $\pi\pi$ and $K\bar{K}$ coupled channel interactions. Some recent works [13,14] studied the interaction of the nonet of vector mesons themselves and found a pole with the quantum number $J^{PC} = 0^{++}$ mainly coupling to the $\bar{K}^*K^*$ channel, possibly corresponding to $f_0(1710)$.

In this paper, we extend the previous study [14] of $f_0(1710)$ by including its coupling to channels of pseudoscalar mesons in addition to vector mesons to see how these more coupled channels influence the result on the $f_0(1710)$ pole and whether its corresponding partial decay widths to these channels of pseudoscalar mesons are compatible with experimental data. Our work is organized as follows. In Sec. II, we outline the formalism to the coupled-channel interaction [15]. In Sec. III, we give our numerical results and discussion with a brief summary at the end.

II. FORMALISM

The interaction Lagrangian among vector mesons and pseudoscalar mesons is given by [16,17]

$$\mathcal{L}_{VPP} = -ig\langle V^\mu [P, \partial_\mu P]\rangle, \tag{1}$$

where the symbol $\langle \ldots \rangle$ stands for the trace in the $SU(3)$ space and the coupling constant $g = M_V/2f_\pi$ with $M_V = 845.66$ MeV, the $SU(3)$-averaged vector-meson mass, and $f_\pi = 92$ MeV as the pion decay constant. The vector field V^μ is

$$V^\mu = \begin{pmatrix} \frac{1}{\sqrt{2}}\rho^0 + \frac{1}{\sqrt{2}}\omega & \rho^+ & K^{*+} \\ \rho^- & -\frac{1}{\sqrt{2}}\rho^0 + \frac{1}{\sqrt{2}}\omega & K^{*0} \\ K^{*-} & \bar{K}^{*0} & \phi \end{pmatrix}^\mu, \tag{2}$$

and the pseudoscalar field P is

$$P = \begin{pmatrix} \frac{1}{\sqrt{2}}\pi^0 + \frac{1}{\sqrt{6}}\eta & \pi^+ & K^+ \\ \pi^- & -\frac{1}{\sqrt{2}}\pi^0 + \frac{1}{\sqrt{6}}\eta & K^0 \\ K^- & \bar{K}^0 & -\frac{2}{\sqrt{6}}\eta \end{pmatrix}. \tag{3}$$

With the Lagrangian given in Eq. (1), we are able to calculate the vector-vector to pseudoscalar-pseudoscalar scattering amplitudes. The Feynman diagrams needed are

*wangzhengli@itp.ac.cn
†zoubs@itp.ac.cn

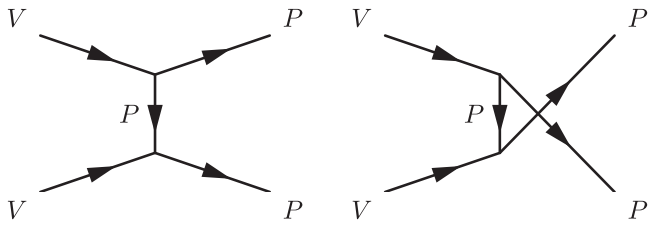

FIG. 1. The t- and u-channel Feynman diagrams.

shown in Fig. 1, where V means vector meson and P means pseudoscalar meson.

The amplitudes with isospin-0 for the processes $V(p_1)V(p_2) \to P(p_3)P(p_4)$ are listed in Table I. The convention used to relate the particle basis to the isospin basis is

$$|\pi^+\rangle = -|1,1\rangle, \qquad |K^+\rangle = -\left|\frac{1}{2},\frac{1}{2}\right\rangle,$$
$$|\rho^+\rangle = -|1,1\rangle, \qquad |K^{*+}\rangle = -\left|\frac{1}{2},\frac{1}{2}\right\rangle. \tag{4}$$

The V_t and V_u correspond to the t- and u-channel diagrams, respectively. The superscript is the particle exchanged. Here, $t = (p_1 - p_3)^2$ and $u = (p_1 - p_4)^2$ are the usual Mandelstam variables. The potential has the form

$$V^{ex}_{t(u)} = \frac{g^2}{t(u) - m^2_{ex}} \epsilon_1 \cdot p_3 \epsilon_2 \cdot p_4, \tag{5}$$

where the ϵ_i is the ith polarization vector of the incoming vector meson. The polarization vector can be characterized by its three-momentum $\mathbf{p}_i$ and the third component of the spin in its rest frame, and the explicit expression of the polarization vectors can be found in Appendix A of Ref. [18].

In term of these amplitudes with isospin-0, we can get the S-wave potential via [18]

$$T^{(JI)}_{\ell S;\bar{\ell}\bar{S}}(s) = \frac{Y^0_\ell(\hat{\mathbf{z}})}{\sqrt{2^N}(2J+1)} \sum_{\substack{\sigma_1,\sigma_2,\bar{\sigma}_1 \\ \bar{\sigma}_2,m}} \int \mathrm{d}\hat{\mathbf{p}}'' Y^m_\ell(\mathbf{p}'')^* (\sigma_1\sigma_2 M|s_1 s_2 S)$$
$$\times (mM\bar{M}|\ell S J)(\bar{\sigma}_1\bar{\sigma}_2\bar{M}|\bar{s}_1\bar{s}_2\bar{S})(0\bar{M}\bar{M}|\bar{\ell}\bar{S}J)$$
$$\times T^{(I)}(p_1,p_2,p_3,p_4;\epsilon_1,\epsilon_2,\epsilon_3,\epsilon_4), \tag{6}$$

with $s = (p_1 + p_2)^2$ as the usual Mandelstam variable, $M = \sigma_1 + \sigma_2$ and $\bar{M} = \bar{\sigma}_1 + \bar{\sigma}_2$. And N accounts for the identical particles, for example

$$N = 2 \quad \text{for } \rho\rho \to \pi\pi, \tag{7}$$

$$N = 1 \quad \text{for } \rho\rho \to K\bar{K}, \tag{8}$$

$$N = 0 \quad \text{for } \omega\phi \to K\bar{K}. \tag{9}$$

Like vector scattering $VV \to VV$, the partial wave projection Eq. (6) for a t-channel exchange amplitude of $VV \to PP$ would also develop a left-hand cut via [14]

$$\frac{1}{2}\int_{-1}^{+1} \mathrm{d}\cos\theta \frac{1}{t - m^2_{ex} + i\epsilon} = -\frac{s}{\sqrt{\lambda(s,m_1^2,m_2^2)\lambda(s,m_3^2,m_4^2)}}$$
$$\times \log \frac{m_1^2 + m_2^2 - \frac{(s+m_1^2-m_2^2)(s+m_3^2-m_4^2)}{2s} - \frac{\sqrt{\lambda(s,m_1^2,m_2^2)\lambda(s,m_3^2,m_4^2)}}{2s} - m^2_{ex} + i\epsilon}{m_1^2 + m_2^2 - \frac{(s+m_1^2-m_2^2)(s+m_3^2-m_4^2)}{2s} + \frac{\sqrt{\lambda(s,m_1^2,m_2^2)\lambda(s,m_3^2,m_4^2)}}{2s} - m^2_{ex} + i\epsilon}, \tag{10}$$

with $\lambda(a,b,c) = a^2 + b^2 + c^2 - 2ab - 2bc - 2ac$ the Källén function. In vector scattering $VV \to VV$, left-hand cuts are smoothed by the N/D method [19,20]. As for the scattering $VV \to PP$, all left-hand cuts are located below the PP threshold, which are far away from the energy region we are interested in, so we do not deal with these cuts.

TABLE I. The potential of each channel with isospin-0.

Channel	$T^{(0)}$
$\rho\rho \xrightarrow{\pi} \pi\pi$	$-16(V_t^\pi + V_u^\pi)$
$\rho\rho \xrightarrow{K} K\bar{K}$	$-2\sqrt{6}(V_t^K + V_u^K)$
$\omega\omega \xrightarrow{K} K\bar{K}$	$2\sqrt{2}(V_t^K + V_u^K)$
$\phi\phi \xrightarrow{K} K\bar{K}$	$4\sqrt{2}(V_t^K + V_u^K)$
$\omega\phi \xrightarrow{K} K\bar{K}$	$-4(V_t^K + V_u^K)$
$K^*\bar{K}^* \xrightarrow{K} \pi\pi$	$-2\sqrt{6}(V_t^K + V_u^K)$
$K^*\bar{K}^* \xrightarrow{K} \eta\eta$	$6\sqrt{2}(V_t^K + V_u^K)$
$K^*\bar{K}^* \xrightarrow{\pi,\eta} K\bar{K}$	$-6(V_t^\pi + V_t^\eta)$

The basic equation to obtain the unitarized T matrix is

$$T^{(JI)}(s) = [1 - V^{(JI)}(s) \cdot G(s)]^{-1} \cdot V^{(JI)}(s). \tag{11}$$

Here $V^{(JI)}$ denotes the partial-wave amplitudes and $G(s)$ is a diagonal matrix made up by the two-point loop function $g_i(s)$,

$$g_i(s) = i \int \frac{\mathrm{d}^4 q}{(2\pi)^4} \frac{1}{(q^2 - m^2_{i1} + i\epsilon)((P-q)^2 - m^2_{i2} + i\epsilon)}, \tag{12}$$

with $P^2 = s$ and $m_{i1,2}$ as the masses of the particles in the ith channel. The pole position is at the zeros of determinant

$$\mathrm{Det} \equiv \det\left[1 - V^{(JI)}(s) \cdot G(s)\right]. \tag{13}$$

The above loop function is logarithmically divergent and can be calculated with a once-subtracted dispersion relation or using a regularization $f_\Lambda(q)$

$$g_i(s) = i \int \frac{\mathrm{d}^4 q}{(2\pi)^4} \frac{f_\Lambda^2(q)}{(q^2 - m_{i1}^2 + i\epsilon)((P-q)^2 - m_{i2}^2 + i\epsilon)}. \tag{14}$$

After the q^0 integration is performed by choosing the contour in the lower half of the complex plane, we get

$$g_i(s) = \int_0^\infty \frac{|\mathbf{q}|^2 \mathrm{d}|\mathbf{q}|}{(2\pi)^2} \frac{\omega_{i1} + \omega_{i2}}{\omega_{i1}\omega_{i2}(s - (\omega_{i1} + \omega_{i2})^2 + \mathrm{i}\epsilon)} f_\Lambda^2(|\mathbf{q}|), \tag{15}$$

where $\mathbf{q}$ is the three-momentum and $\omega_{i1,2} = \sqrt{\mathbf{q}^2 + m_{i1,2}^2}$. In order to proceed we need to determine $f_\Lambda(\mathbf{q})$. There are two kinds of choices, sharp cutoff and smooth cutoff, typically:

$$f_\Lambda(\mathbf{q}) = \begin{cases} \Theta(\Lambda^2 - \mathbf{q}^2) \\ \exp\left[-\frac{\mathbf{q}^2}{\Lambda^2}\right] \end{cases}. \tag{16}$$

In order to compare with the previous results of coupled channel approach [14], the same sharp cutoff is used in this paper when channels with pseudoscalar mesons are included in addition. To explore the position of the poles, we need to take into account the analytical structure of these amplitudes in the different Riemann sheets. By denoting q_{on} for the CM trimomentum of the particles 1 and 2 in the ith channel

$$q_i^{\mathrm{on}} = \frac{\sqrt{(s - (m_{i1} - m_{i2})^2)(s - (m_{i1} + m_{i2})^2)}}{2\sqrt{s}}. \tag{17}$$

As the quantity is two valued itself [21], we need to distinguish the two Riemann sheets of q_i^{on} uniquely according to

$$q_i^{\mathrm{on}>} = \begin{cases} -q_i^{\mathrm{on}} & \text{if } \mathrm{Im} q_i^{\mathrm{on}} < 0 \\ q_i^{\mathrm{on}} & \text{else} \end{cases}. \tag{18}$$

And the analytic continuation to the second Riemann sheet is given by

$$g_i^{(2)}(s) = g_i(s) + \frac{i}{4\pi} \frac{q_i^{\mathrm{on}>}}{\sqrt{s}}. \tag{19}$$

III. NUMERICAL RESULTS AND DISCUSSION

First we assume that $f_0(1710)$ is $K^*\bar{K}^*$ hadron molecule state and calculate the partial decay widths of $f_0(1710) \to K^*\bar{K}^* \to \pi\pi, K\bar{K}, \eta\eta$ with the hadronic triangle loop approach [22–25], as shown in Fig. 2.

The loop function corresponding to this process as shown in Fig. 2 is

$$D = -i \int \frac{\mathrm{d}^4 q}{(2\pi)^4} \frac{1}{(p_3 + q)^2 - m_{K^*}^2 + i\epsilon} \times \frac{1}{(p_4 - q)^2 - m_{\bar{K}^*}^2 + i\epsilon} \frac{1}{q^2 - m_3^2 + i\epsilon}, \tag{20}$$

where for different final state m_3 can be the mass of π, K, η. Since the mass of $f_0(1710)$ is close to the threshold of $K^*\bar{K}^*$, the internal lines with K^* and $\bar{K}^*$ exchange can be approximated nonrelativistically. And the loop function can be simplified as

$$D = -i \int \frac{\mathrm{d}^4 q}{(2\pi)^4} \frac{1}{4m_{K^*}^2} \frac{1}{(p^0 - \omega_1)^2 - (q^0)^2 - i\epsilon} \times \frac{1}{(q^0)^2 - \omega_3^2 + i\epsilon} \left(\frac{\Lambda^2 - m_{ex}^2}{\Lambda^2 - q^2}\right)^2 \exp\left[-\frac{(\mathbf{p}+\mathbf{q})^2}{\Lambda_G^2}\right], \tag{21}$$

with $p_3 = (p^0, \mathbf{p}), q = (q^0, \mathbf{q})$, $\omega_1 = \sqrt{(\mathbf{p} + \mathbf{q})^2 + m_{K^*}^2}$, and $\omega_3 = \sqrt{\mathbf{q}^2 + m_3^2}$. Here for the vertex $f_0(1710)K^*\bar{K}^*$ the Gaussian form factor is added. For the t-channel meson exchange, coupling constants with an off shell meson are dressed by monopole form factors [26,27]. For simplicity, we take Λ_G and Λ to be equal to be in the range of 0.8–1.0 GeV. And the results are

$$\frac{\Gamma(f_0(1710) \to \pi\pi)}{\Gamma(f_0(1710 \to K\bar{K}))} = 0.394 \pm 0.134 \quad (0.23 \pm 0.05), \tag{22}$$

$$\frac{\Gamma(f_0(1710) \to \eta\eta)}{\Gamma(f_0(1710 \to K\bar{K}))} = 0.239 \pm 0.057 \quad (0.48 \pm 0.15), \tag{23}$$

where the values of the PDG [28] are given between brackets. It seems that the calculated partial decay width of $f_0(1710) \to \pi\pi$ is larger than the central value in PDG, but it is still within the range of large error bar.

To check how the $f_0(1710)$ is influenced by various coupled channels in the unitary coupled channel approach,

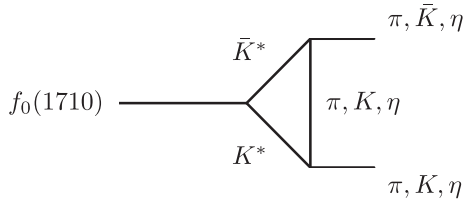

FIG. 2. Decay of $f_0(1710)$.

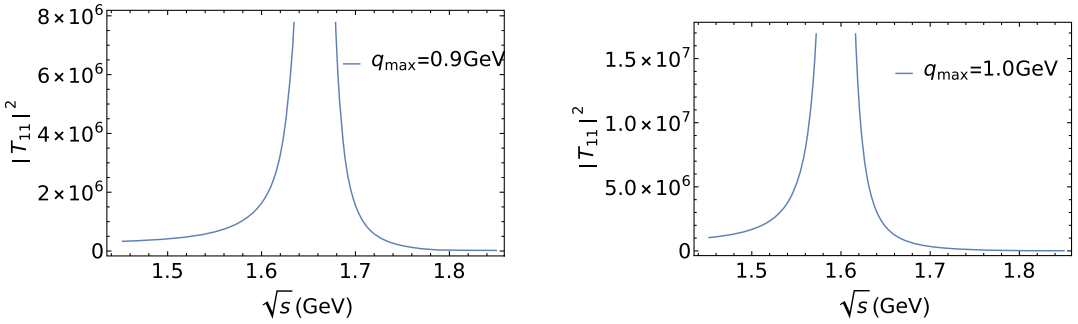

FIG. 3. $|T_{11}|^2$ for different $q_{\max} = 0.9$, 1.0 GeV.

we start with the single $K^*\bar{K}^*$ channel case by dropping its couplings to all other channels. The Fig. 3 gives the $|T|^2$ matrix of scattering $K^*\bar{K}^* \to K^*\bar{K}^*$. We label the $K^*\bar{K}^*$ as channel 1, and the remain channel indices are listed in Table II. A bound state is found locating at $\sqrt{s} = 1.66$ GeV for cutoff $q_{\max} = 0.9$ GeV and $\sqrt{s} = 1.60$ GeV for $q_{\max} = 1.0$ GeV. The bound state moves down when the cutoff $q_{\max}$ increases, similar to the case for the $\rho\rho$ bound states [29]. This is understandable that the smaller $q_{\max}$ value gives a stronger cutoff to the loop integration to reduce the attractive force.

Then we turn on additional channels to study their influence on the mass and width of the resonance. The T matrix for a single channel a is given by

$$T_{aa} = \frac{V_{aa}}{1 - V_{aa}g_a}. \tag{24}$$

If we turn on another channel b, then the T matrix for $a \to a$ becomes

$$T_{aa} = \frac{V_{aa} + \frac{V_{ab}^2 g_b}{1 - V_{bb}g_b}}{1 - (V_{aa} + \frac{V_{ab}^2 g_b}{1 - V_{bb}g_b})g_a}. \tag{25}$$

Compared to the single channel, V_{aa} is replaced by

$$V_{\text{eff}} = V_{aa} + \frac{V_{ab}^2 g_b}{1 - V_{bb}g_b}. \tag{26}$$

TABLE II. Channel indices and threshold energies.

Channel index	Channel	Threshold (GeV)
1	$K^*\bar{K}^*$	1.784
2	$\rho\rho$	1.54
3	$\omega\omega$	1.564
4	$\phi\phi$	2.04
5	$\omega\phi$	1.802
6	$K\bar{K}$	0.99
7	$\pi\pi$	0.276
8	$\eta\eta$	1.096

Denoting the second term as

$$V' = \frac{V_{ab}^2 g_b}{1 - V_{bb}g_b}, \tag{27}$$

then T_{aa} can be written as

$$T_{aa} = \frac{V_{aa} + V'}{1 - (V_{aa} + V')g_a} = \frac{(1+\alpha)V_{aa}}{1 - (1+\alpha)V_{aa}g_a}. \tag{28}$$

with $\alpha = V'/V_{aa}$. For calculating the loop integral g_a for channels of vector mesons, we use the same sharp cutoff as in the previous study [14]. However, if we turn on the channels of pseudoscalar mesons, the t-channel exchanged pseudoscalar meson in $VV \to PP$ is mostly off shell for the calculation of V', and the implementation of some off shell form factors is necessary [29]. Adjustment of the sharp cutoff parameter $q_{\max}$ for the loop integration has no influence for the imaginary part of g_b, which corresponds to two on shell pseudoscalar mesons with an off shell t-channel exchanged pseudoscalar meson. To take into account this off shell effect of the t-channel exchanged meson, the same kind of monopole form factor as in our triangle loop approach as well as in Ref. [29]

$$F = \frac{\Lambda^2 - m_{ex}^2}{\Lambda^2 - q^2} \tag{29}$$

is included at each VPP vertex for the exchanged pseudoscalar meson with momentum q. For the $VV \to PP$ process, the t-channel exchange meson is much more off shell than corresponding $VV \to VV$ case. The off shell suppression effect makes V_{ab} to be a few times smaller than V_{aa}, so that $|\alpha| \ll 1$ and the inclusion of the pseudoscalar channels does not change much the previous result.

When the form factor is implemented, the T matrix for $K^*\bar{K}^* \to \eta\eta$ is showed in Fig. 4. For cutoff $q_{\max} = 0.9$ GeV, the real part of the resonance is around 1.66 GeV, which is the same as the single channel. The imaginary part is about 6,14,26 MeV for different $\Lambda = 0.8$, 0.9, 1.0 GeV. And for cutoff $q_{\max} = 1.0$ GeV, the situation is similar.

For the $K^*\bar{K}^* - K\bar{K}$ system, the $|T|^2$ is showed in Fig. 5. The resonance is $\sqrt{s} = 1.76 - 0.015i$ GeV for

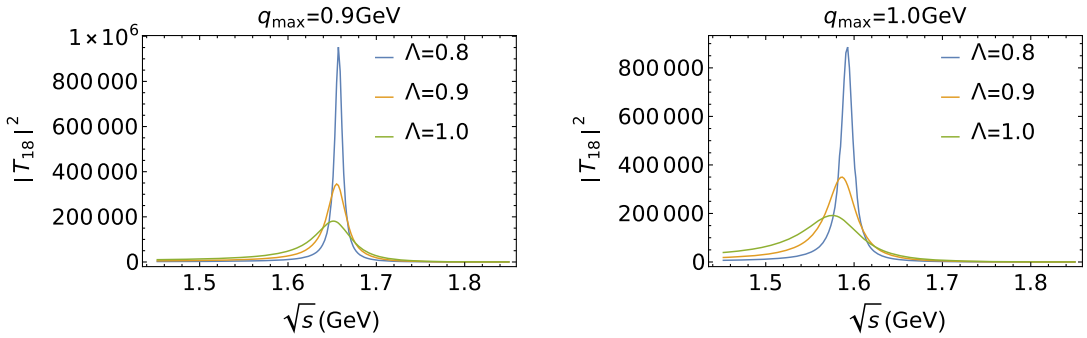

FIG. 4. $|T_{18}|^2$ for different $\Lambda = 0.8$, 0.9, 1.0 GeV and $q_{\max} = 0.9$, 1.0 GeV.

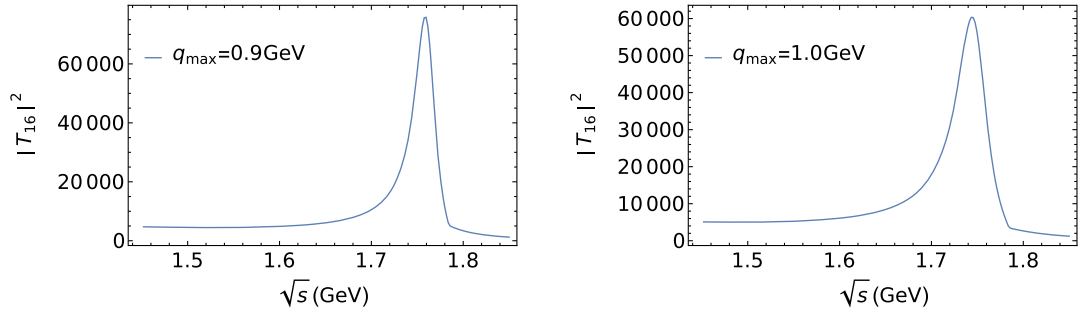

FIG. 5. $|T_{16}|^2$ for $\Lambda = 0.9$ GeV and different $q_{\max} = 0.9$, 1.0 GeV.

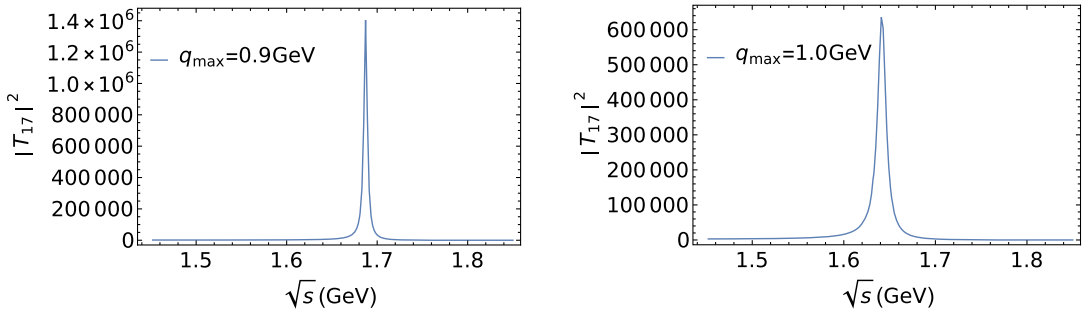

FIG. 6. $|T_{17}|^2$ for $\Lambda = 0.9$ GeV and different $q_{\max} = 0.9$, 1.0 GeV.

$q_{\max} = 0.9$ GeV and $\sqrt{s} = 1.75 - 0.022i$ GeV for $q_{\max} = 1.0$ GeV. Compared to the single channel, turning on the $K\bar{K}$ channel makes the resonance moving up along the real axis. And the situation is similar for $K^*\bar{K}^* - \pi\pi$ system, see Fig. 6. The resonance is at $\sqrt{s} = 1.69 - 0.004i$ GeV for $q_{\max} = 0.9$ GeV and $\sqrt{s} = 1.64 - 0.007i$ GeV and $q_{\max} = 1.0$ GeV. We find the width of the resonance in $K^*\bar{K}^* - \eta\eta$ system is about equivalence to

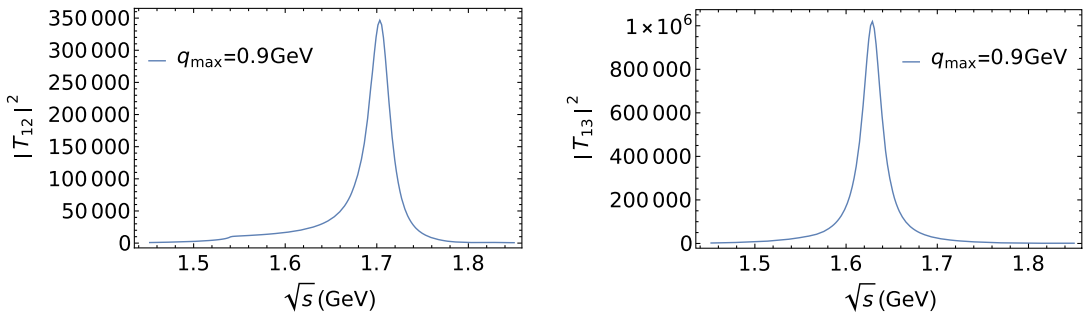

FIG. 7. $|T_{12}|^2$ and $|T_{13}|^2$ for $\Lambda = 0.9$ GeV and $q_{\max} = 0.9$ GeV.

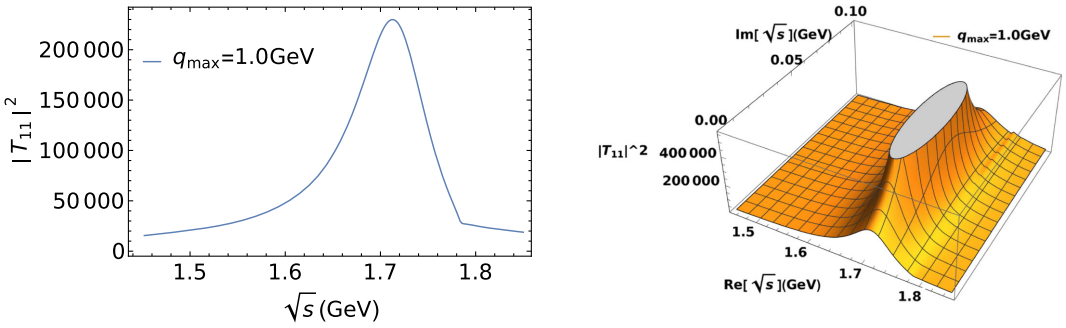

FIG. 8. $|T_{11}|^2$ for $\Lambda = 0.9$ GeV and $q_{\max} = 1.0$ GeV in 2-dim and 3-dim.

that in $K^*\bar{K}^* - \pi\pi$ system, and about $2 \sim 3$ times smaller than that in the $K^*\bar{K}^* - K\bar{K}$ system. For comparison, we also show the $|T|^2$ for $K^*\bar{K}^* - \rho\rho$ and $K^*\bar{K}^* - \omega\omega$ system, see Fig. 7. The resonance is about $\sqrt{s} = 1.70 - 0.014i$ GeV for $K^*\bar{K}^* - \rho\rho$ and $\sqrt{s} = 1.63 - 0.013i$ GeV for $K^*\bar{K}^* - \omega\omega$ with the cutoff $q_{\max} = 0.9$ GeV. It is interesting that turning on the $\omega\omega$ channel makes the pole to move down, recall that the pole is at 1.66 GeV for $K^*\bar{K}^*$ single channel. Actually we find that if there is no interaction for the additional channel, such as $V(\omega\omega \to \omega\omega) = 0$, $V(\eta\eta \to \eta\eta) = 0$, the pole moves down in the coupled channel, otherwise, the pole moves up along the real axis.

Finally, we turn on all channels and show the $|T_{11}|^2$ in 2-dim and 3-dim with $q_{\max} = 1.0$ GeV in Fig. 8. The position of the resonance is listed in Table III for different cutoffs. We find that the real part of resonance is about 1710 MeV and the width is about 100 MeV, quite close to the PDG values for the $f_0(1710)$ with mass 1704 ± 12 MeV and width 123 ± 18 MeV [28]. Up to now, we have ignored the width of K^* which is about 50 MeV. Similar to the case for the $\rho\rho$ molecules studied in Ref. [29], the finite width of K^* does not influence the bind energy of $\bar{K}^*K^*$ molecule much, but it increases the width of the molecule by the direct decays of both $\bar{K}^*$ and K^*. With the effective coupling constant of $f_0(1710)\bar{K}^*K^*$ determined by its binding energy, the partial decay width of $f_0(1710) \to \bar{K}^*K^* \to K\pi\bar{K}\pi$ can be calculated straightforwardly to be around 21 MeV, which makes the total width of $f_0(1710)$ in perfect agreement with its PDF value. This means that the $f_0(1710)$ can be dynamically generated by mesons scattering. And we also find the lower resonance at $1.46 - 0.012i$ GeV for $q_{\max} = 1.0$ GeV and $1.48 - 0.008i$ GeV for $q_{\max} = 0.875$ GeV. Compared to our previous work [30], the resonance move down a little along the real axis, which is $1.52 - 0.009i$ GeV for $q_{\max} = 1.0$ GeV and $1.53 - 0.005i$ GeV for $q_{\max} = 0.875$ GeV in [30].

For the unitary coupled channel approach, we can calculate the ratio of decay width via [28]

$$\Gamma_{R\to a} = \frac{|\tilde{g}_a|^2}{M_R}\rho_a(M_R^2), \tag{30}$$

with $\tilde{g}_a = \mathcal{R}_{ba}/\sqrt{\mathcal{R}_{bb}}$ and ρ_a as the two-body phase space. The residues may be calculated via an integration along a closed contour around the pole using

$$\mathcal{R}_{ba} = -\frac{1}{2\pi i}\oint ds\mathcal{M}_{ba}. \tag{31}$$

The branching ratios obtained this way are

$$\frac{\Gamma(f_0(1710) \to \pi\pi)}{\Gamma(f_0(1710 \to K\bar{K}))} = 0.289 \pm 0.092 \quad (0.23 \pm 0.05), \tag{32}$$

$$\frac{\Gamma(f_0(1710) \to \eta\eta)}{\Gamma(f_0(1710 \to K\bar{K}))} = 0.294 \pm 0.048 \quad (0.48 \pm 0.15), \tag{33}$$

where the values of the PDG [28] are given in the brackets at the end of each equation for comparison. In fact the deviation from various collaborations is much larger than the PDG range: the value of $\Gamma(f_0(1710) \to \pi\pi)/\Gamma(f_0(1710 \to K\bar{K}))$ is $0.64 \pm 0.27 \pm 0.18$ in [31], $0.41^{+0.11}_{-0.17}$ in [32], $0.2 \pm 0.024 \pm 0.036$ in [33], 0.39 ± 0.14 in [34], and 0.32 ± 0.14 in [35]. The value of $\Gamma(f_0(1710) \to \eta\eta)/\Gamma(f_0(1710 \to K\bar{K}))$ is 0.48 ± 0.15 in [36] and $0.46^{+0.70}_{-0.38}$ in [37]. And for the radiative decays of J/ψ in Table IV from PDG [28], all we can say is that the partial decay widths of $f_0(1710) \to \pi\pi$ and $f_0(1710) \to \eta\eta$

TABLE III. The resonance pole for different cutoffs.

$q_{\max}$(GeV)	0.7	0.8	0.9	1.0	1.1
Pole(GeV)	1.77–0.015i	1.75–0.028i	1.73–0.035i	1.72–0.045i	1.70–0.053i

TABLE IV. Some modes of radiative decays of J/ψ.

Mode	Fraction(Γ_i/Γ)
$\gamma f_0(1710) \to \gamma K\bar{K}$	$9.5^{+1.0}_{-0.5} \times 10^{-4}$
$\gamma f_0(1710) \to \gamma\pi\pi$	$3.8^{+0.5}_{-0.5} \times 10^{-4}$
$\gamma f_0(1710) \to \gamma\eta\eta$	$2.4^{+1.2}_{-0.7} \times 10^{-4}$

are similar to be around $1/3$ of $f_0(1710) \to K\bar{K}$, which are compatible with our results.

In summary, we extend the coupled channel interaction of nonet of vectors by including channels of the octet of pseudoscalars in addition using the unitary coupled-channel approach. The pole near the $K^*\bar{K}^*$ threshold remains to be there with mass and width consistent with PDG values of $f_0(1710)$. Meanwhile we deduce the partial decay widths of $f_0(1710) \to K^*\bar{K}^* \to \pi\pi, K\bar{K}, \eta\eta$ in the approach as well as hadronic triangle loop approach for hadronic molecule. In both cases, the results agree with that of $f_0(1710)$ in PDG. We can conclude that the properties of $f_0(1710)$ are consistent with the $K^*\bar{K}^*$ molecule state. Previously, as a candidate of glueball, the $f_0(1710)$ has been extensively studied within the quarkonia-guleball mixing picture [35,38–43]. With the success of the new possible configuration as hadron molecule to explain its decays, the structure of $f_0(1710)$ could be beyond the quarkonia-guleball mixing picture and need further exploration by including the new possible configuration to fit its various relevant properties, not only decays, but also various productions.

ACKNOWLEDGMENTS

We thank useful discussions and valuable comments from Feng-Kun Guo, Ulf-G. Meißner and Jia-Jun Wu. This work is supported by the NSFC and the Deutsche Forschungsgemeinschaft (DFG, German Research Foundation) through the funds provided to the Sino-German Collaborative Research Center TRR110 Symmetries and the Emergence of Structure in QCD (NSFC Grant No. 12070131001, DFG Project-ID 196253076-TRR 110), by the NSFC Grants No. 11835015 and No. 12047503, and by the Chinese Academy of Sciences (CAS) under Grant No. XDB34030000.

[1] F. K. Guo, C. Hanhart, U. G. Meißner, Q. Wang, Q. Zhao, and B. S. Zou, Rev. Mod. Phys. **90**, 015004 (2018).
[2] X. K. Dong, F. K. Guo, and B. S. Zou, Prog. Phys. **41**, 65 (2021).
[3] J. Oller, E. Oset, and J. Pelaez, Phys. Rev. D **62**, 114017 (2000).
[4] J. Oller and U. G. Meißner, Phys. Lett. B **500**, 263 (2001).
[5] A. Dobado and J. Pelaez, Phys. Rev. D **56**, 3057 (1997).
[6] J. Oller and E. Oset, Phys. Rev. D **60**, 074023 (1999).
[7] J. Oller, E. Oset, and J. Pelaez, Phys. Rev. D **59**, 074001 (1999).
[8] J. Oller and E. Oset, Nucl. Phys. **A620**, 438 (1997).
[9] J. Oller, E. Oset, and A. Ramos, Prog. Part. Nucl. Phys. **45**, 157 (2000).
[10] R. Molina and E. Oset, Phys. Lett. B **811**, 135870 (2020).
[11] D. Jido, J. Oller, E. Oset, A. Ramos, and U. Meissner, Nucl. Phys. **A725**, 181 (2003).
[12] G. Janssen, B. Pearce, K. Holinde, and J. Speth, Phys. Rev. D **52**, 2690 (1995).
[13] L. S. Geng and E. Oset, Phys. Rev. D **79**, 074009 (2009).
[14] M. L. Du, D. Glmez, F. K. Guo, U. G. Meißner, and Q. Wang, Eur. Phys. J. C **78**, 988 (2018).
[15] J. A. Oller, Prog. Part. Nucl. Phys. **110**, 103728 (2020).
[16] M. Bando, T. Kugo, S. Uehara, K. Yamawaki, and T. Yanagida, Phys. Rev. Lett. **54**, 1215 (1985).
[17] M. Bando, T. Kugo, and K. Yamawaki, Phys. Rep. **164**, 217 (1988).
[18] D. Gülmez, U. G. Meißner, and J. A. Oller, Eur. Phys. J. C **77**, 460 (2017).
[19] G. F. Chew and S. Mandelstam, Phys. Rev. **119**, 467 (1960).
[20] J. Bjorken, Phys. Rev. Lett. **4**, 473 (1960).
[21] M. Doring, C. Hanhart, F. Huang, S. Krewald, and U. G. Meißner, Nucl. Phys. **A829**, 170 (2009).
[22] M. L. Du, V. Baru, F. K. Guo, C. Hanhart, U. G. Meißner, J. A. Oller, and Q. Wang, Phys. Rev. Lett. **124**, 072001 (2020).
[23] Y. H. Lin and B. S. Zou, Phys. Rev. D **100**, 056005 (2019).
[24] F. K. Guo, H. J. Jing, U. G. Meißner, and S. Sakai, Phys. Rev. D **99**, 091501 (2019).
[25] Y. H. Lin, C. W. Shen, F. K. Guo, and B. S. Zou, Phys. Rev. D **95**, 114017 (2017).
[26] R. Machleidt, Adv. Nucl. Phys. **19**, 189 (1989).
[27] A. I. Titov, B. Kampfer, and B. L. Reznik, Eur. Phys. J. A **7**, 543 (2000).
[28] P. A. Zyla *et al.* (Particle Data Group), Prog. Theor. Exp. Phys. **2020**, 083C01 (2020).
[29] R. Molina, D. Nicmorus, and E. Oset, Phys. Rev. D **78**, 114018 (2008).
[30] Z. L. Wang and B. S. Zou, Phys. Rev. D **99**, 096014 (2019).
[31] J. P. Lees *et al.* (*BABAR* Collaboration), Phys. Rev. D **97**, 112006 (2018).
[32] M. Ablikim, J. Z. Bai, Y. Ban, J. G. Bian, X. Cai, H. F. Chen, H. S. Chen, H. X. Chen, J. C. Chen, J. Chen *et al.*, Phys. Lett. B **642**, 441 (2006).

[33] D. Barberis *et al.* (WA102 Collaboration), Phys. Lett. B **462**, 462 (1999).
[34] T. A. Armstrong *et al.* (WA76 Collaboration), Z. Phys. C **51**, 351 (1991).
[35] M. Albaladejo and J. A. Oller, Phys. Rev. Lett. **101**, 252002 (2008).
[36] D. Barberis *et al.* (WA102 Collaboration), Phys. Lett. B **479**, 59 (2000).
[37] V. V. Anisovich, V. A. Nikonov, and A. V. Sarantsev, Phys. At. Nucl. **65**, 1545 (2002).
[38] F. E. Close, G. R. Farrar, and Z. P. Li, Phys. Rev. D **55**, 5749 (1997).
[39] F. E. Close and Q. Zhao, Phys. Rev. D **71**, 094022 (2005).
[40] F. Giacosa, T. Gutsche, V. E. Lyubovitskij, and A. Faessler, Phys. Rev. D **72**, 094006 (2005).
[41] M. Chanowitz, Phys. Rev. Lett. **95**, 172001 (2005).
[42] K. T. Chao, X. G. He, and J. P. Ma, Phys. Rev. Lett. **98**, 149103 (2007).
[43] M. Albaladejo and J. A. Oller, Phys. Rev. Lett. **101**, 252002 (2008).